Low Bandgap Polymers Based on Silafluorene Containing Multifused Heptacylic Arenes for Photovoltaic Applications

ARTICLE *in* MACROMOLECULES · AUGUST 2012

Impact Factor: 5.8 · DOI: 10.1021/ma300839c

Macromolecules

Article

pubs.acs.org/Macromolecules

Low Bandgap Polymers Based on Silafluorene Containing Multifused Heptacylic Arenes for Photovoltaic Applications

Mingjian Yuan,[†] Pinyi Yang,[†] Matthew M. Durban,[‡] and Christine K. Luscombe*[,†]

[†]Materials Science and Engineering Department, University of Washington, Seattle, Washington 98195-2120, United States

[‡]Department of Chemistry, University of Washington, Seattle, Washington 98195-1750, United States

Supporting Information

ABSTRACT: A series of donor−acceptor copolymers based on a new silafluorene containing multifused heptacylic arenes have been designed and synthesized in order to further modulate and optimize their electronic and optical properties. Polymer solar cells based on a blend of these polymers and $PC_{61}BM$ exhibited high open circuit voltages of up to 0.86 V. Through simple and straightforward engineering of molecular structures, the devices based on the PSiFDCTBT:$PC_{61}BM$ (1:3.5 in wt %) blend provided, on average, a V_{oc} of 0.86 V, a J_{sc} of 8.8 mA/cm^2, a FF of 56%, delivering a PCE of 4.2%.

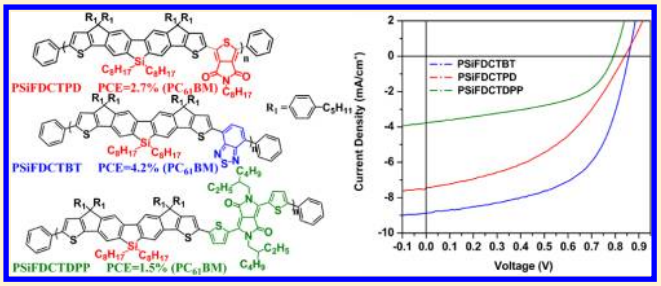

INTRODUCTION

Polymer solar cells (PSCs) have attracted increased attention due to their potential application toward flexible, large-area, and low-cost photovoltaic devices.[1] Since the introduction of the bulk heterojunction (BHJ) concept, significant efforts have been put forth to improve the power conversion efficiency (PCE) to meet the criterion of high performance photovoltaic applications.[2] Very recently, efficiencies higher than 8% have been achieved by several groups, which shows great potential for commercialization.[3]

To achieve highly efficient PSCs, conjugated polymers with relatively low band gaps, high absorption-coefficients, balanced HOMO and LUMO energy levels, good solubility, and appropriate miscibility with fullerene derivatives in blended active-layers are important prerequisites. Extensive π-conjugation of a rigid polymer backbone will facilitate intermolecular interactions between polymer chains and increase the charge mobility of the polymers.[4] Recently, several ladder-type copolymers have been investigated for achieving efficient PSCs.[5] Specifically, silole-containing semiconducting polymers have been known to exhibit altered properties with respect to their carbon analogues. A variety of functionalized silole-containing semiconducting polymers have been reported to show promising characteristics as materials for PSCs.[6,7] The silole(silacyclopentadiene) moiety has been investigated as a system where the σ*-orbital of the silicon−carbon bond interacts with the π*-orbital of the butadiene fragment resulting in a lower lying LUMO.[7a] The research groups of Yang and Brabec have independently shown that replacing the bridging carbon atom in cyclopenta[2,1-*b*;3,4-*b*′]dithiophene containing polymers with silicon helps to increase the crystallinity of the polymers[7b,c] providing polymers that have relatively high charge carrier mobilities.[7d] Studies have also indicated that these silicon bridged polymers have good environmental stability.[7e]

In considering the above, we have designed and synthesized a new variety of low bandgap copolymers that contain a multifused thienyl−fluorene−thienyl subunit where the bridging carbon atom on the fluorine has been replaced with a silicon atom. Forced planarization by covalently fastening adjacent aromatic units within the polymer backbone helps to strengthen parallel π-orbital interactions to extend the effective conjugation length and facilitate π-electron delocalization, providing an effective way to reduce the band gap. Moreover, coplanar geometries and rigid structures can suppress rotational disorder around interannular single bonds and lower the reorganization energy, which can in turn enhance intrinsic charge mobilities.[8]

In order to further modulate and optimize the electronic and optical properties, exploration of different electron-deficient units incorporated into multifused thienyl-fluorene-thienyl based polymeric backbone is highly desirable. Benzothiadiazole (BT) and thieno[3,4-*c*]pyrrole-4,6-dione (PD) units are widely used electron-deficient units introduced in the D−A copolymers due to their suitable electron affinity and easy synthesis.[9] In addition, diketopyrrolopyrrole (DPP) has also emerged as a useful acceptor unit because of its planar conjugated bicyclic structure and strong electron-withdrawing nature of polar amide group.[10] On the basis of the modified multifused thienyl−fluorene−thienyl as the core structure, we have successfully synthesized three D−A copolymers, PSiFDCTPD, PSiFDCTBT, and PSiFDCTDPP (Scheme 1). The synthesis, characterization, and photovoltaic applications of these polymers will be discussed.

Received: April 25, 2012
Revised: July 19, 2012
Published: July 27, 2012

Scheme 1. Synthetic Route for the SiFDCT Monomer and the Corresponding Copolymers

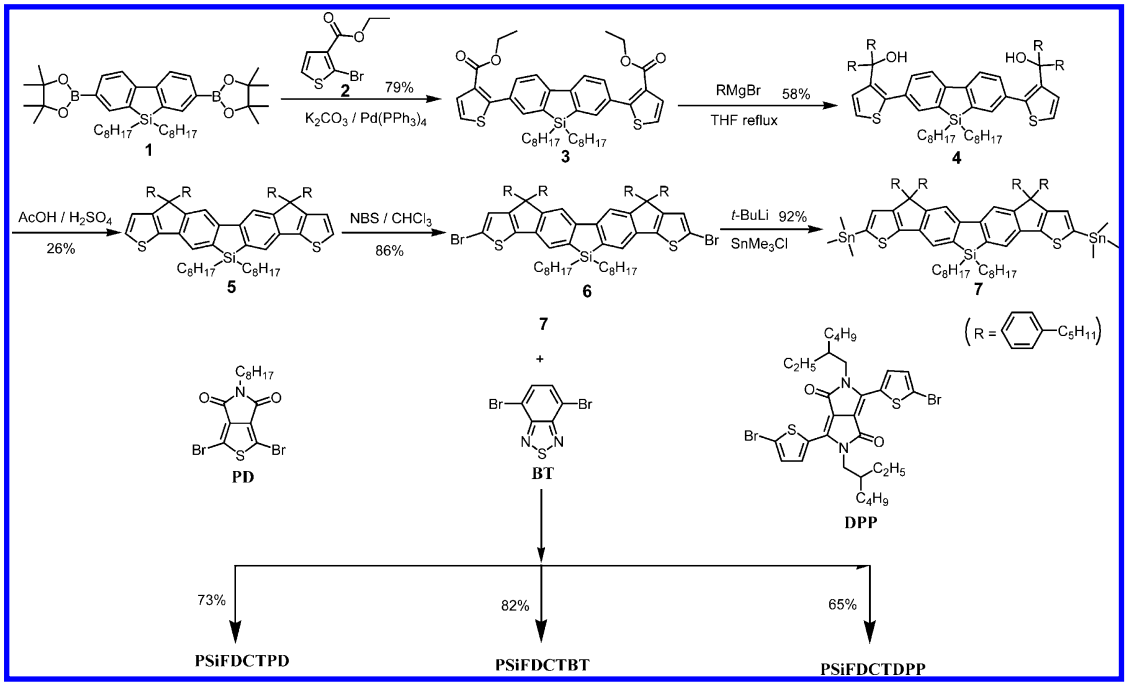

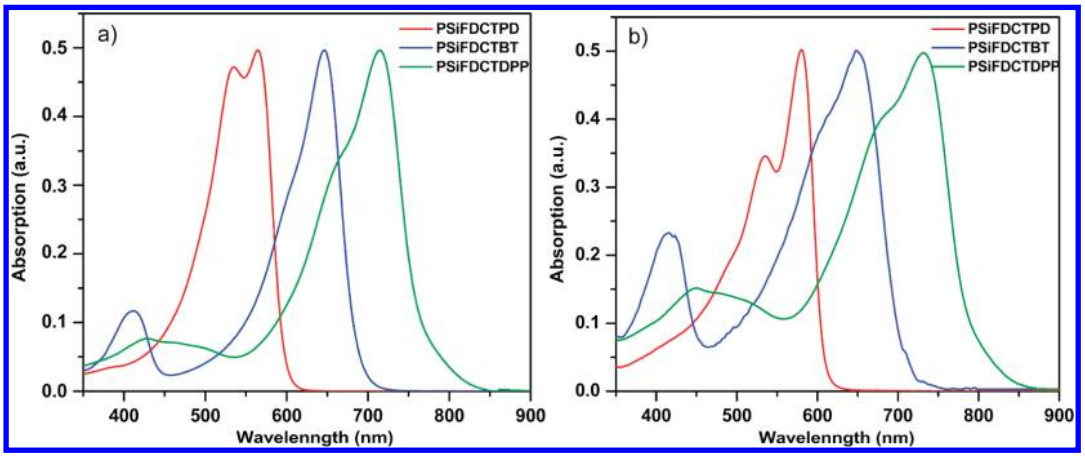

Figure 1. Normalized absorption spectra of PSiFDCTPD, PSiFDCTBT, PSiFDCTDPP in chloform (a) and as a thin film (b).

RESULTS AND DISCUSSION

Synthesis and Characterization. The synthetic route of the SiFDCT monomer **5** is depicted in Scheme 1. Suzuki coupling of 2,7-diboronic ester silafluorene **1** with ethyl 2-bromothiophene-3-carboxylate afforded compound **3**. Double nucleophilic addition of freshly prepared 4-(*n*-pentyl)-phenylmagnesium bromide to the ester groups of compound **3** led to the formation of tertiary benzylic alcohol compound **4**, which was subjected to intramolecular annulation through Lewis acid-mediated Friedel–Crafts reaction to furnish SiFDCT **5**. A bulky aromatic substituent was used instead of flexible aliphatic chains for solubilization for synthetic ease.[5e] SiFDCT **5** was brominated in $CHCl_3$ to yield compound **6** in good yield. Treatment of compound **6** with *t*-butyl lithium followed by quenching with trimethyltin chloride successfully afforded the distannyl compound **7**. Compound **7** was then copolymerized with 1,3-dibromo-5-octylthieno[3,4-*c*]pyrrole-4,6-dione (PD), 4,7-dibromo-2,1,3-benzothiadiazole (BT), and 3,6-bis(5-bromothiophene-2-yl)-2,5-bis[(2-ethyl)hexyl]-pyrrolo[3,4-*c*]pyrrole-1,4-dione (DPP), by Stille coupling to give **PSiFDCTPD** (M_n = 16.3 kDa, PDI = 2.1), **PSiFDCTBT** (M_n = 37.4 kDa, PDI = 2.5), and **PSiFDCTDPP** (M_n = 10.4 kDa, PDI = 1.6), respectively. The structures of the polymers were determined by NMR spectroscopy. All polymers showed excellent solubilities in common organic solvents, such as chloroform, toluene and dichlorobenzene.

Optical Properties. As shown in Figure 1a, the absorption spectra of the three polymers in dilute chloroform exhibited two characteristic bands. Each polymer has an absorption band located between 300 and 550 nm with a second broad absorption from 500 to 800 nm. The shorter wavelength absorption can be attributed to the $\pi-\pi^*$ transition of the heptacylic units, while the lower energy band can be attributed to the intramolecular charge transfer (ICT) between the electron-rich and electron-deficient segments.[11] Compared to PSiFDCTPD, which shows absorption maxima at 535 and 562 nm in solution, PSiFDCTBT exhibited an absorption maximum at 410 nm with a bathochromic shift of the ICT band to 646 nm. PSiFDCTDPP exhibited an absorption maximum at 430 nm with the ICT band at 714 nm. From Figure 1b, the

dx.doi.org/10.1021/ma300839c | *Macromolecules* 2012, 45, 5934–5940

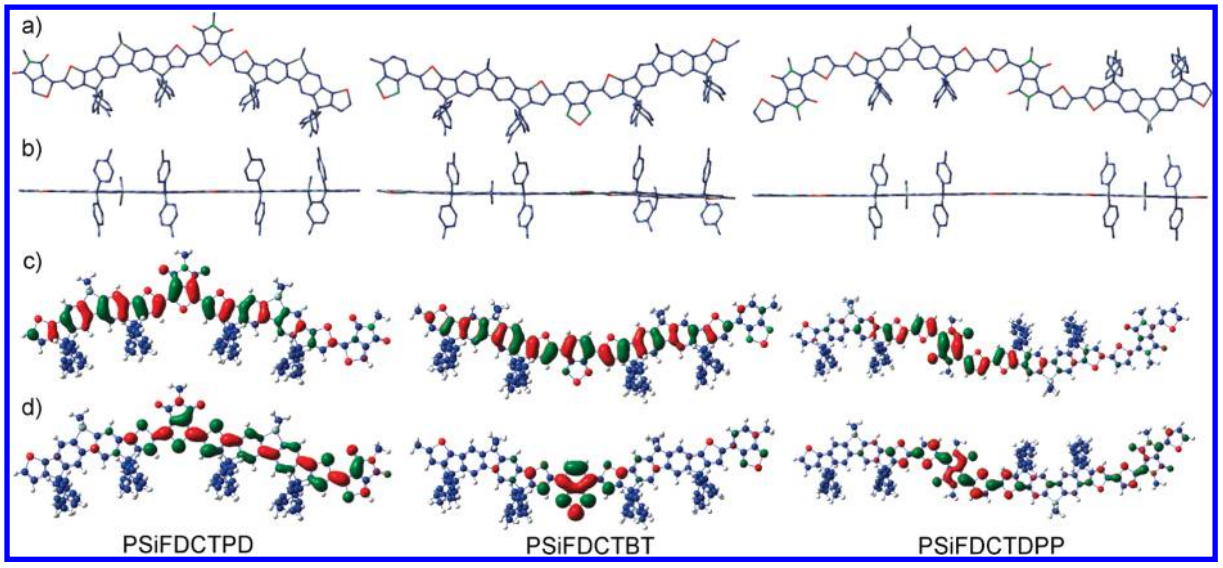

Figure 2. Optimized conformations for the structure of PSiFDCTPD, PSiFDCTBT, PSiFDCTDPP top view (a) and side view (b). Wave functions of the HOMO (c) and LUMO (d) orbitals of the corresponding polymers calculated at the level of B3LYP/6-31G (d,p).

absorption of all the polymers shifted toward longer wavelengths from solution to the solid state, indicating that the planar structure of SiFDCT is capable of inducing strong interchain interactions. The optical band-gaps (E_g^{opt}) deduced from the absorption edges of the thin film spectra are in the following order: PSiFDCTPD (1.88 eV) > PSiFDCTBT (1.76 eV) > PSiFDCTDPP (1.57 eV). The difference of their absorption maxima as well as E_g^{opt} indicates that the acceptor strength is in the order DPP > BT > DP.[12] Note that the intensities of the shorter wavelength bands of the polymer in the solid state are apparently stronger than those in the solution state, which suggests that the rigid and coplanar nonacyclic units can enhance their light absorption ability in the solid state.

Theoretical Calculations. To further understand the effect of planarization on the molecular structures and properties, we performed theoretical calculations by density functional theory at the level of B3LYP/6-31G(d). Two repeating units SiFDCTPD, SiFDCTBT, and SiFDCTDPP were used as simplified models for simulation of the corresponding three copolymers. Methyl groups were used in the approximation of long alkyl chains in order to reduce calculation time. The optimized structures for PSiFDCTPD, PSiFDCTBT, and PSiFDCTDPP are shown in Figure 2. All three polymers show planar conformations through the entirety of the polymer backbone. The dihedral angles between the acceptor moieties and the neighboring SiFDCT fused-ring are $\sim\varphi = 0°$.

The frontier orbitals of the model compounds SiFDCTPD, SiFDCTBT, and SiFDCTDPP are shown in Figure 2. The calculated HOMO energy levels of SiFDCTPD, SiFDCTBT, and SiFDCTDPP were −5.54, −5.72, and −5.68 eV, respectively, which are in general agreement with the experimentally determined values for the corresponding polymers (see cyclic voltammetry measurements below) albeit with a shift of 0.2−0.4 eV. For the corresponding alternating dimers, the electron density of the LUMO was primarily located on the electron-accepting unit (Figure 2d), whereas the electron density of the HOMO was more evenly distributed across both the donor and acceptor with the exception of PSiFDCTDPP (Figure 2c). This redistribution of electron density shows a pronounced intramolecular charge separation between the donor and acceptor following excitation.

Electrochemical Properties. Cyclic voltammetry (CV) was employed to investigate the electrochemical properties and evaluate the HOMO and LUMO energy levels of the individual polymers (Figure S1, Suuporting Information). The HOMO and LUMO energy levels were calculated from the onset oxidation potentials (E_{onset}^{ox}) and onset reduction potentials (E_{onset}^{red}) vs Ag/Ag^+, respectively, according to eqs 1 and 2.

$$\text{HOMO} = -(E_{ox} + 4.75)\ (\text{eV}) \quad (1)$$

$$\text{LUMO} = -(E_{red} + 4.75)\ (\text{eV}) \quad (2)$$

The electrochemically determined band gaps were deduced from the difference of the onset oxidation and reduction potentials. The energy levels are summarized in Figure 3.

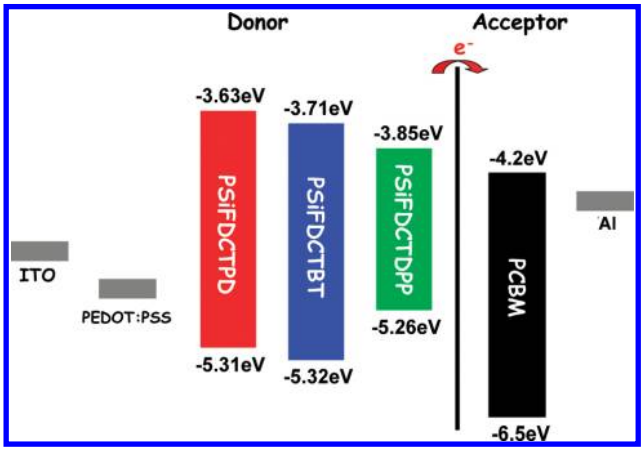

Figure 3. Energy level diagrams for PSiFDCTPD, PSiFDCTBT, and PSiFDCTDPP.

All of the polymers showed one stable and reversible p-doping and n-doping processes, which are important prerequisites for p-type semiconductor materials. The HOMO energy levels were estimated to be −5.31 eV for PSiFDCTPD, −5.32 eV for PSiFDCTBT, and −5.26 eV for PSiFDCTDPP, which are in an ideal range to ensure improved air stability and greater attainable V_{oc} in the final device. The

dx.doi.org/10.1021/ma300839c | Macromolecules 2012, 45, 5934−5940

Table 1. Photovoltaic and Hole-Mobility Characterization

	mobility ($cm^2/(V·s)$)						
		blend					
	polymer	hole	electron	V_{oc} (V)	J_{sc} (mA/cm^2)	FF (%)	PCE (%)
PSiFDCTPD	1.0×10^{-8}	2.5×10^{-6}	1.2×10^{-8}	0.84	7.3 ± 0.1	44 ± 1	2.7 ± 0.1
PSiFDCTBT	1.0×10^{-8}	5.4×10^{-5}	4.8×10^{-8}	0.86	8.8 ± 0.2	56 ± 1	4.2 ± 0.1
PSiFDCTDPP	1.1×10^{-8}	4.6×10^{-7}	3.1×10^{-8}	0.79	3.78 ± 0.02	49.5 ± 0.3	1.48 ± 0.02

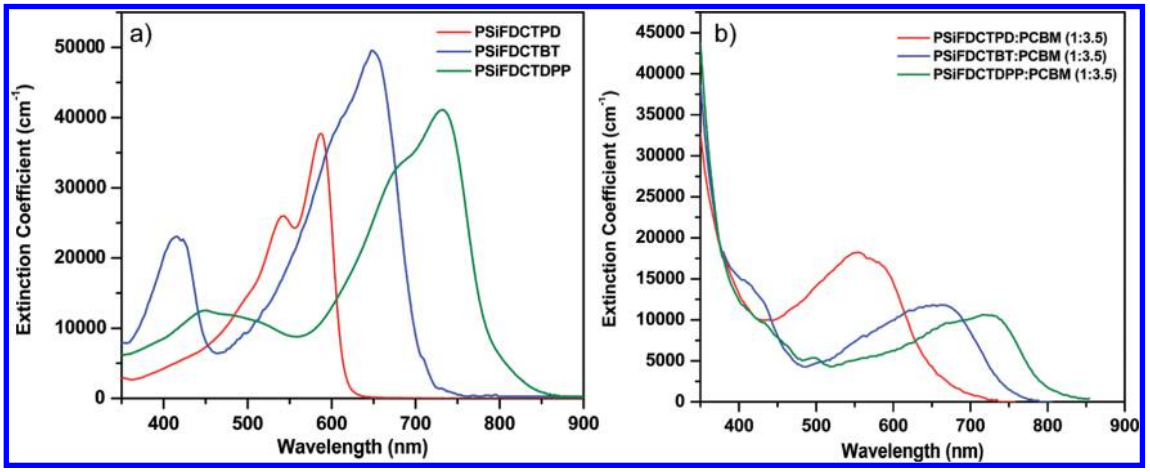

Figure 4. (a) Absorption spectra of PSiFDCTPD, PSiFDCTBT, and PSiFDCTDPP pure polymer films. (b) Absorption spectra of PSiFDCTPD:$PC_{61}BM$, PSiFDCTBT:$PC_{61}BM$, and PSiFDCTDPP:$PC_{61}BM$ blends films.

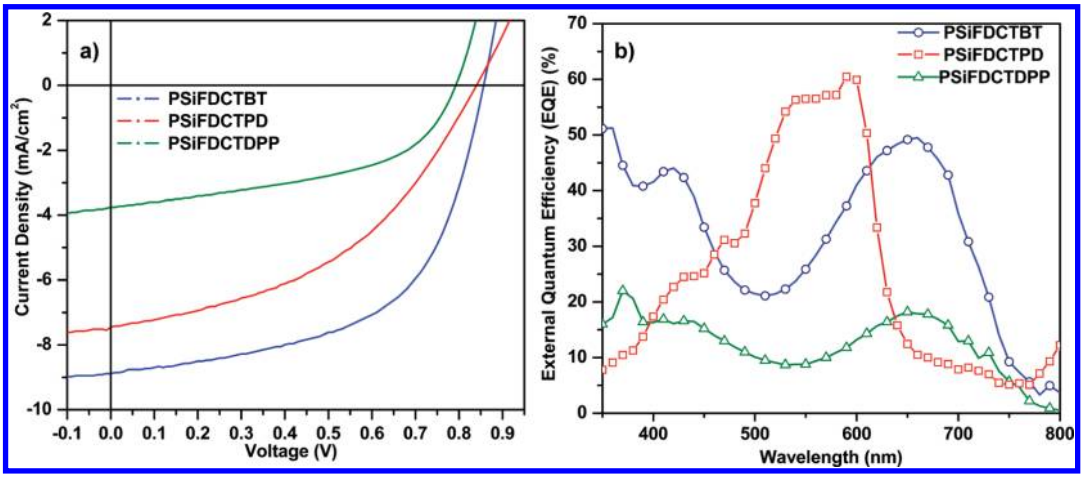

Figure 5. (a) $J-V$ characteristics of ITO/PEDOT:PSS/polymer:$PC_{61}BM$/Al under illumination of AM 1.5, 100 mW/cm^2. (b) EQE characteristics of the same devices.

LUMO energy levels are approximately located at −3.63 eV for PSiFDCTPD and −3.71 eV for PSiFDCTBT, which are much higher than the LUMO level of the $PC_{61}BM$ acceptor (−4.2 eV) to ensure energetically favorable electron transfer.

Photovoltaic and Hole-Mobility Characteristics. BHJ photovoltaic cells were fabricated by spin-coating the blend from chlorobenzene (CB) solutions at optimized polymer:$PC_{61}BM$ (1:3.5) ratios using a ITO/PEDOT:PSS/polymer:$PC_{61}BM$/Al device configuration with an active layer of approximately 100 nm. Device performances were measured under a simulated AM 1.5 G illumination of 100 mW/cm^2. Additionally, in order to evaluate the hole and electron mobility in the pure film and active-layer blend by space-charge limited current (SCLC) theory, devices with appropriate configurations (see Experimental Section for details; Figures S5−S7, Supporting Information) were fabricated. The device data are summarized in Table 1.

The hole mobilities of all three polymers prior to blending with $PC_{61}BM$ were similar at around 1.0×10^{-8} $cm^2/(V\ s)$. However, after blending with $PC_{61}BM$, the hole mobilities of the blended films exhibited an improvement in performance several orders of magnitude higher than the pure films. This phenomenon has been reported by others[13] and is most likely due to the intercalation of $PC_{61}BM$ between the polymer side chains, which in turn inhibits coiling of the polymer chains. The planarization of the polymer backbone is said to increase the conjugation length, improves intermolecular interactions, and improves charge mobilities. In Figure 4b, which shows the absorption spectra of the blended films, we see a red-shift in the absorption spectra compared to the pure polymer films (Figure

dx.doi.org/10.1021/ma300839c | Macromolecules 2012, 45, 5934−5940

4a) confirming the increased planarity of the polymers upon blending. The hole mobilities of the blended films followed the trend PSiFDCTDPP:$PC_{61}BM$ (4.6×10^{-7} $cm^2/(V\ s)$) < PSiFDCTPD:$PC_{61}BM$ (2.5×10^{-6} $cm^2/(V\ s)$) < PSiFDCTBT:$PC_{61}BM$ (5.4×10^{-5} $cm^2/(V\ s)$), which may indicate that the side chains on PSiFDCTBT are spaced in such a way as to provide improved intercalation of $PC_{61}BM$ compared to the side chains of PSiFDCTPD and PSiFDCTDPP.[14,15] Looking at the absorption spectra in Figure 4, PSiFDCTBT does indeed show the greatest red-shift when blended with $PC_{61}BM$ indicating that it undergoes the greatest degree of planarization upon blending in this particular series of polymers.

The *J-V* and external quantum efficiency characteristics of the devices are shown in Figure 5. High V_{oc} values were obtained from all devices. As the V_{oc} can be linearly correlated with the difference between the HOMO level of electron donor (polymers) and the LUMO of electron acceptor ($PC_{61}BM$),[16] the V_{oc} values matched the expected values calculated from the energy levels of polymer materials.

In order to investigate the lower PCE of PL spectra of all three polymers with and without $PC_{61}BM$ were taken (Figures S2−S4, Supporting Information). Both PSiFDCTPD:$PC_{61}BM$ and PSiFDCTBT:$PC_{61}BM$ blends exhibited over 90% PL quenching, whereas only 20% PL quenching was observed in blends consisting of PSiFDCTDPP:$PC_{61}BM$ showing that less charge transfer is occurring in the latter devices. This is the primary justification for that devices fabricated using PSiFDCTDPP:$PC_{61}BM$ showing a much lower J_{sc} (3.8 mA/cm^2) and PCE (1.5%) than devices fabricated from the other polymer:$PC_{61}BM$ blends.

The highest performing devices were found from solar cells fabricated from PSiFDCTBT:$PC_{61}BM$ blends, with a PCE of 4.2% (V_{oc} = 0.86 V, J_{sc} = 8.8 mA/cm^2, FF = 56%). Devices fabricated from PSiFDCTPD:$PC_{61}BM$ under the same processing conditions only showed a PCE of 2.7%. From the EQE spectra it can be seen that although PSiFDCTPD:$PC_{61}BM$ achieved the highest maximum value of approximately 65%, PSiFDCTBT:$PC_{61}BM$ showed a broader profile and higher average EQE values. At short wavelengths, the EQEs of PSiFDCTBT:$PC_{61}BM$ blends were about 2 to 3 times higher than the other two active layer blends. This may be one reason why PSiFDCTBT:$PC_{61}BM$ devices showed a higher overall PCE than PSiFDCTPD:$PC_{61}BM$ and PSiFDCTDPP:$PC_{61}BM$ devices. Moreover, it has been shown that achieving a balance between the hole and electron mobilities in organic solar cells is one of the key issues in obtaining high-performance devices.[17] The similar electron and hole mobilities in PSiFDCTBT:$PC_{61}BM$ (Table 1) may be another reason for their improved device performance.

CONCLUSION

We have successfully designed and synthesized a ladder-type multifused thienyl-fluorene-thienyl unit with rigid and coplanar backbone. The distannyl SiFDCT building block was copolymerized with electron-deficient thieno[3,4-*c*]pyrrole-4,6-dione (PD), benzothiadiazole (BT), and dithienyldiketo-pyrrolopyrrole (DPP) units by Stille polymerization to afford three alternating donor−acceptor copolymers, PSiFDCTPD, PSiFDCTBT and PSiFDCTDPP respectively. Through simple and straightforward engineering of molecular structures, the device based on the PSiFDCTBT:$PC_{61}BM$ (1:3.5) blend performed a V_{oc} of 0.86 V, a J_{sc} of 8.8 mA/cm^2, and a FF of 56%, delivering a PCE of 4.2%. The corresponding PSiFDCTBT:$PC_{61}BM$ blend also showed a high hole mobility of 5.4×10^{-5} $cm^2/(V\ s)$, leading to a high current density and fill factor.

EXPERIMENTAL SECTION

General Measurement and Characterization. All chemicals were purchased from Aldrich or VWR and used as received unless otherwise specified. Compound **1**[18] and the corresponding PD,[9] BT,[19] and DPP[10] monomers were synthesized according to previous literature procedures. ^1H NMR and ^{13}C NMR spectra were collected on a Brüker Avance DPS-300 spectrometer. Mass spectrometry was performed using a Hewlett-Packard 5971A gas chromatograph and Brüker Biflex III MALDI−TOF (both positive and negative ion reflector mode). The molecular weight of the polymers was measured using Viscotek TDA 305 with polystyrene standards (room temperature, THF as eluent). The absorption spectra were measured using a Perkins-Elmer Lambda-9 spectrophotometer. Cyclic voltammetry of the polymer films was conducted in acetonitrile with 0.1 M of tetrabutylammonium hexafluorophosphate using a scan rate of 100 mV s^{-1}. ITO, Ag/AgCl, and Pt mesh were used as the working electrode, reference electrode, and counter electrode, respectively.

Fabrication and Characterization of BHJ Devices. ITO/Glass substrates were ultrasonically cleaned sequentially in detergent, water, acetone, and isopropyl alcohol. The substrates were covered by a 30 nm layer of PEDOT:PSS by spin coating. After annealing in air at 140 °C for 10 min, the samples were cooled to room temperature. Polymers were dissolved in CB and $PC_{61}BM$ was added to reach the optimized ratio (1:3.5). The solutions were then heated at 90 °C and stirred overnight. Prior to deposition, the solutions were filtered through a 0.2 μm filter and the substrates were transferred into a glovebox. The photoactive layer was then spin coated at different speeds to get a thickness about 100 nm. The aluminum cathode (100 nm thick) was thermally evaporated through a shadow mask under high vacuum about 4.0×10^{-7} Torr. Devices were then transferred outside the glovebox to test in air using a Keithley 2400 source measurement unit, and an Oriel xenon lamp (450 W) coupled with an AM1.5 filter was used as the light source. The light intensity was calibrated with a calibrated standard silicon solar cell with a KG5 filter which is traced to the National Renewable Energy Laboratory and a light intensity of 100 mW·cm^{-2} was used in all the measurements in this study. Devices parameters were obtained by taking the average of 15 samples for PSiFDCTBT and 7−8 samples for PSiFDCTPD and PSiFDCTDPP. Theoretical short circuit currents and mismatch factors have been calculated and are shown in Table S1, Supporting Information.

Hole-Only Devices. To investigate the hole mobility of polymer films, we chose specific top and bottom contact electrodes in order to measure the charge mobilities within our films (pure film, ITO/PEDOT:PSS/polymer/Al; blends films, electron mobility; ITO/Al/polymer:$PC_{61}BM$/Al; hole mobility, ITO/PEDOT:PSS/polymer:$PC_{61}BM$/Pd). The hole mobilities were calculated according to space charge limited current theory (SCLC). The *J*−*V* curves were fitted according to the following equation:

$$J_{e(h)} = \frac{9}{8}\varepsilon_0\varepsilon_r\mu_{e(h)}\exp\left(0.891\gamma_{e(h)}\sqrt{\frac{V}{L}}\right)\frac{V^2}{L^3}$$

Here $J_{e(\eta)}$ is the electron (hole) current, $\mu_{e(h)}$ the zero-field mobility of the electrons (holes), $\gamma_{e(h)}$ the field activation factor, ε_0 the permittivity of free space, ε_r the relative permittivity of the material, and L the thickness of the active layer. The current was measured by Keithley 2400 source measurement unit. Polymer mobility was gained from the best fitted device.

Synthesis of Compound 3. To a 50 mL two-neck flask was introduced compound **1** (2.54 g, 3.86 mmol), ethyl 2-bromothiophene-3-carboxylate (2.35 g, 10 mmol), $Pd(PPh_3)_4$ (230 mg, 0.2 mmol, K_2CO_3 (2.76 g, 20 mmol), and Aliquat 336 (200 mg, 0.5 mmol) in a solution of degassed toluene (30 mL), and degassed H_2O

dx.doi.org/10.1021/ma300839c | *Macromolecules* 2012, 45, 5934−5940

(5 mL). The mixture was heated to 90 °C under nitrogen overnight. The resulting solution was extracted with ethyl acetate and washed with brine. The combined organic layer was dried over Na_2SO_4. After removal of the solvent under reduced pressure, the residue was purified by column chromatography on silica gel (hexane/ethyl acetate, v/v, 25:1) to give compound **3** as a sticky liquid (2.18 g, 79%). ^{1}H NMR (300 MHz, $CDCl_3$): 7.81 (d, 2H), 7.48 (d, 2H), 7.53−7.46 (m, 4H), 7.22 (d, 2H), 4.21 (m, 4H), 1.98 (m, 4H), 1.21−1.11 (t, 30H), 0.88 (t, 6H). ^{13}C NMR (75 MHz, $CDCl_3$): 158.29, 151.03, 150.86, 140.45, 138.75, 134.62, 130.05, 129.47, 125.21, 124.97, 120.59, 56.32, 42.76, 34.61, 31.77, 30.20, 30.16, 25.36, 23.21, 14.52, 14.26. MS (MALDI−TOF): m/z ($C_{42}H_{54}O_4S_2Si$) calcd, 714.3; found, 713.8.

Synthesis of Compound 4. To a solution of 4-pentyl-1-bromobenzene (2.73 g, 12 mmol) in anhydrous THF under nitrogen was added *n*-BuLi (4.8 mL, 12 mmol, 2.5 M) dropwise at −78 °C. The resulting solution was stirred for 1 h at this temperature. Then a solution of compound **3** (1.43 g, 2 mmol) in anhydrous THF was added slowly to the above solution. After the addition, the resulting mixture was heated at reflux overnight. The resulting mixture was extracted with ethyl acetate and washed with brine. The combined organic layer was dried over Na_2SO_4. After removal of the solvent under reduced pressure, the residue was purified by column chromatography on silica gel (chloroform) to give compound **4** as a sticky liquid (1.41 g, 58%). ^{1}H NMR (300 MHz, $CDCl_3$): 7.46 (d, 2H), 7.23 (d, 2H), 7.19 (m, 8H), 7.12 (d, 2H), 7.08 (m, 8H), 7.02 (s, 2H), 6.79 (d, 2H), 3.02 (s, 2H), 1.98−1.67 (m, 4H), 1.57−0.80 (m, 74H). ^{13}C NMR (75 MHz, $CDCl_3$): 154.13, 150.62, 145.23, 139.87, 139.45, 138.21, 132.92, 132.12, 129.85, 128.56, 125.02, 121.78, 120.15, 113.53, 74.32, 36.21, 32.48, 32.14, 30.55, 29.93, 29.51, 28.76, 25.26, 24.77, 24.39, 22.64, 15.36, 12.85. MS (MALDI−TOF): m/z ($C_{82}H_{106}O_2S_2Si$) calcd, 1214.7; found, 1213.6.

Synthesis of Compound 5. To a solution of compound **4** (2.5 g, 2 mmol) in acetic acid (150 mL) was added concentrated H_2SO_4 (3 mL) in one portion. The resulting mixture was refluxed for 4 h and then was extracted with ethyl acetate and washed with brine. The combined organic layer was dried over Na_2SO_4. After removal of the solvent under reduced pressure, the residue was purified by silica gel chromatograph with hexane as the eluent to give a yellow oil product compound **5** (630 mg, 26%). ^{1}H NMR (300 MHz, $CDCl_3$): 7.51 (s, 2H), 7.38 (s, 2H), 7.21 (d, 2H), 7.14 (m, 8H), 7.09 (m, 8H), 6.88 (d, 2H), 1.96−1.69 (m, 4H), 1.60−0.80 (m, 74H). ^{13}C NMR (75 MHz, $CDCl_3$): 156.34, 155.07, 152.46, 149.53, 142.12, 138.76, 137.23, 134.68, 129.94, 128.04, 125.01, 120.45, 117.39, 114.05, 75.16, 37.01, 33.21, 33.04, 31.39, 30.18, 30.01, 29.34, 25.97, 25.01, 24.84, 22.21, 16.24, 15.72. MS (MALDI−TOF): m/z ($C_{82}H_{102}S_2Si$) calcd, 1178.7; found, 1177.1.

Synthesis of Compound 6. Compound **5** (500 mg, 0.42 mmol) was dissolved in chloroform (15 mL), and then NBS (167 mg, 0.92 mmol) was added into the solution at 0 °C. The resulting mixture was stirred at room temperature for another 2 h. Then the solution was poured onto a sodium carbonate solution (2 M) and extracted with chloroform. The organic phase was dried over anhydrous Na_2SO_4, the solvent was removed under reduced pressure, and the residue was purified by silica gel chromatograph with hexane as the eluent to get compound **6** as a yellow solid (482 mg, 86%). ^{1}H NMR (300 MHz, $CDCl_3$): 7.53 (s, 2H), 7.39 (s, 2H), 7.19 (m, 8H), 7.12 (m, 8H), 7.06 (s, 2H), 1.94−1.62 (m, 4H), 1.60−0.75 (m, 74H). ^{13}C NMR (75 MHz, $CDCl_3$): 157.25, 155.46, 153.01, 150.11, 144.29, 139.31, 138.07, 134.47, 128.72, 127.96, 124.31, 121.25, 118.26, 114.67, 75.31, 38.53, 34.07, 33.26, 31.35, 31.09, 30.78, 30.01, 26.45, 25.72, 24.68, 22.53, 16.85, 15.31. MS (MALDI−TOF): m/z ($C_{82}H_{100}Br_2S_2Si$) calcd, 1334.5; found, 1333.2.

Synthesis of Compound 7. Compound **6** (400 mg, 3 mmol) and anhydrous THF were added to a flask under nitrogen atmosphere and cooled to −78 °C. Subsequently, *n*-butyllithium (3 mL, 7.5 mmol, 2.5 M) was added dropwise into the solution. After stirring at −78 °C for 1 h, trimethyltin chloride (7.5 mL, 7.5 mmol, 1 M) was added into the solution in one portion. The resulting solution was stirred at room temperature for another 1 h. The solution was poured onto water and extracted with diethyl ether twice. The organic phase was dried over anhydrous Na_2SO_4, the solvent was removed under reduced pressure. The residue was washed with cold methanol and then dried under high vacuum overnight to give compound **7** as a white solid (416 mg, 92%). ^{1}H NMR (300 MHz, $CDCl_3$): 7.48 (s, 2H), 7.31 (s, 2H), 7.17 (m, 8H), 7.11 (m, 8H), 6.97 (s, 2H), 1.96−1.60 (m, 4H), 1.50−0.75 (m, 74H), 0.39 (s, 18H). ^{13}C NMR (75 MHz, $CDCl_3$): 155.68, 154.01, 153.64, 149.23, 143.52, 140.16, 138.75, 135.35, 129.13, 128.43, 125.14, 122.35, 119.37, 112.14, 76.23, 42.12, 35.63, 34.28, 32.38, 32.17, 31.59, 30.42, 30.21, 29.58, 28.74, 26.21, 25.84, 25.13, 23.08, 17.13 16.20. MS (MALDI−TOF): m/z ($C_{88}H_{118}S_2SiSn_2$) calcd, 1506.7; found, 1507.4.

General Synthetic Procedure for PSiFDCTPD, PSiFDCTBT, and PSiFDCTDPP by Stille Coupling Reaction. All of the polymers were prepared by a similar procedure. To a Schlenk flask was introduced compound **7** (753.5 mg, 0.5 mmol), corresponding acceptor monomer (0.5 mmol), and anhydrous chlorobenzene (4 mL). The solution was flushed with nitrogen for 10 min, and then a catalytic amount of tris(dibenzylideneacetone) dipalladium(0) (8.6 mg, 3 mol %) and tri(*o*-tolyl)phosphine (22.9 mg, 15 mol %) was added into the solution. After the resulting flask was degassed thrice via a freeze−pump−thaw cycle, the reactants were heated up to 100 °C for 48 h. Then, the reaction was cooled to room temperature and added into methanol dropwise. The precipitate was collected by filtration and washed by Soxhlet extraction with methanol, acetone, hexane, and chloroform. The chloroform fraction was then concentrated and precipitated into methanol. The solid was filtered and dried under vacuum for 1 day.

Polymer PSiFDCTPD. Red solid; yield 73%. ^{1}H NMR (300 MHz, $CDCl_3$): 8.01 (br, 2H), 7.41 (m, 2H), 7.26 (m, 8H), 7.08(m, 8H), 6.74 (m, 2H), 3.09 (br, 4H), 2.87 (br, 2H), 2.08−0.72 (m, 93H). M_n = 16.3K; PDI = 2.1; M_w = 34.2K.

Polymer PSiFDCTBT. Red-blue solid; yield 82%. ^{1}H NMR (300 MHz, $CDCl_3$): 8.08 (br, 2H), 7.75 (br, 2H), 7.52 (m, 2H), 7.19 (m, 8H), 7.10 (m, 8H), 6.87 (m, 2H), 3.14 (br, 4H), 2.03−0.71 (m, 78H). M_n = 37.4K; PDI = 2.5; M_w = 93.5K.

Polymer PSiFDCTDPP. Green solid; yield 65%. ^{1}H NMR (300 MHz, $CDCl_3$): 8.23 (br, 2H), 7.61 (br, 4H), 7.36 (m, 2H), 7.22 (m, 8H), 7.14 (m, 8H), 6.81 (m, 2H), 3.25 (br, 4H), 2.95 (br, 4H), 2.12−0.83 (m, 104H). M_n = 10.4K; PDI = 1.6; M_w = 16.6K.

■ ASSOCIATED CONTENT

Supporting Information

Cyclic voltammograms of the corresponding polymer, fluorescent emission spectra of the corresponding polymer and blend, hole/electron mobility fitting plots for the polymers and blends, ^{1}H NMR spectra of the copolymers, and table of mismatch factors. This material is available free of charge via the Internet at http://pubs.acs.org.

■ AUTHOR INFORMATION

Corresponding Author

*E-mail: luscombe@u.washington.edu.

Present Address

†Materials Science and Engineering Department, University of Washington, Seattle, Washington 98195−2120

Author Contributions

The manuscript was written through the contributions of all authors. All authors have given approval to the final version of the manuscript. .

Notes

The authors declare no competing financial interest.

■ ACKNOWLEDGMENTS

This work was supported by the NSF (STC-MDITR DMR 0120967, SOLAR Award DMR 1035196, EFRI-SEED 1038165, and CAREER Award DMR 0747489).

REFERENCES

(1) Tang, C. W. *Appl. Phys. Lett.* **1986**, *48*, 183.
(2) Yu, G.; Gao, J.; Hummelen, J. C.; Wudl, F.; Heeger, A. J. *Science* **1995**, *270*, 1789.
(3) (a) Chen, H.-Y.; Hou, J.; Zhang, S.; Liang, Y.; Yang, G.; Yang, Y.; Yu, L.; Wu, Y.; Li, G. *Nature Photonics.* **2009**, *3*, 649. (b) He, Z.; Zhong, C.; Huang, X.; Wong, W.; Wu, H.; Chen, L.; Su, S.; Cao, Y. *Adv. Mater.* **2011**, *23*, 4636.
(4) (a) Du, C.; Li, C.; Li, W.; Chen, X.; Bo, Z.; Veit, C.; Ma, Z.; Wuerfel, U.; Zhu, H.; Hu, W.; Zhang, F. *Macromolecules* **2011**, *44*, 7617. (b) Yuan, M.; Okamoto, K.; Bronstein, H. A.; Luscombe, C. K. *ACS Macro Lett.* **2012**, *1*, 392. (c) Wang, E.; Ma, Z.; Zhang, Z.; Vandewal, K.; Henriksson, P.; Inganäs, O.; Zhang, F.; Andersson, M. R. *J. Am. Chem. Soc.* **2011**, *133*, 14244. (d) Zhou, E.; Cong, J.; Tajima, K.; Hashimoto, K. *Chem. Mater.* **2010**, *22*, 4890.
(5) (a) Cheng, Y.-J.; Wu, J.-S.; Shih, P.-I.; Chang, C.-Y.; Jwo, P.-C.; Kao, W.-S.; Hsu, C.-S. *Chem. Mater.* **2011**, *23*, 2361. (b) Cheng, Y.-J.; Chen, C.-H.; Lin, Y.-S.; Chang, C.-Y.; Hsu, C.-S. *Chem. Mater.* **2011**, *23*, 5068. (c) Cheng, Y.-J.; Ho, Y.-J.; Chen, C.-H.; Kao, W.-S.; Wu, C.-E.; Hsu, S.-L.; Hsu, C.-S. *Macromolecules* **2012**, *45*, 2690. (d) Cheng, Y.-J.; Cheng, S.-W.; Chang, C.-Y.; Kao, W.-S.; Liao, M.-H.; Hsu, C.-S. *Chem. Commun.* **2012**, *48*, 3203. (e) Chang, C.-Y.; Cheng, Y.-J.; Hung, S.-H.; Wu, J.-S.; Kao, W.-S.; Lee, C.-H.; Hsu, C.-S. *Adv. Mater.* **2012**, *24*, 549.
(6) (a) Wang, J.-Y.; Hau, S. K.; Yip, H.-L.; Davies, J. A.; Chen, K.-S.; Zhang, Y.; Sun, Y.; Jen, A. K.-Y. *Chem. Mater.* **2011**, *23*, 765. (b) Ashraf, R. S.; Chen, Z.; Leem, D. S.; Bronstein, H.; Zhang, W.; Schroeder, B.; Geerts, Y.; Smith, J.; Watkins, S.; Anthopoulos, T. D.; Sirringhaus, H.; de Mello, J. C.; Heeney, M.; McCulloch, I. *Chem. Mater.* **2011**, *23*, 768.
(7) (a) Zhan, X.; Risko, C.; Amy, F.; Chan, C.; Zhao, W.; Barlow, S.; Kahn, A.; Bredas, J.-L.; Marder, S. R. *J. Am. Chem. Soc.* **2005**, *127*, 9021. (b) Chen, H.-Y.; Hou, J.; Hayden, A. E.; Yang, H.; Houk, K. N.; Yang, Y. *Adv. Mater.* **2010**, *22*, 371. (c) Morana, M.; Azimi, H.; Dennler, G.; Egelhaaf, H.-J.; Scharber, M.; Forberich, K.; Hauch, J.; Gaudiana, R.; Waller, D.; Zhu, Z.; Hingerl, K.; van Bavel, S. S.; Loos, J.; Brabec, C. J. *Adv. Funct. Mater.* **2010**, *20*, 1180. (d) Usta, H.; Lu, G.; Facchetti, A.; Marks, T. J. *J. Am. Chem. Soc.* **2006**, *128*, 9034. (e) Hou, J.; Chen, H.-Y.; Zhang, S.; Li, G.; Yang, Y. *J. Am. Chem. Soc.* **2008**, *130*, 16144.
(8) (a) Cheng, Y.-J.; Yang, S.-H.; Hsu, C.-S. *Chem. Rev.* **2009**, *109*, 5868. (b) Zhou, H.; Yang, L.; You, W. *Macromolecules* **2012**, *45*, 607.
(9) (a) Zou, Y.; Najari, A.; Berrouard, P.; Beaupré, S.; Réda Aïch, B.; Tao, Y.; Leclerc, M. *J. Am. Chem. Soc.* **2010**, *132*, 5330. (b) Piliego, C.; Holcombe, T. W.; Douglas, J. D.; Woo, C. H.; Beaujuge, R. M.; Fréchet, J. M. *J. Am. Chem. Soc.* **2010**, *132*, 7595−7597.
(10) (a) He, C.; He, Q.; Yang, X.; Wu, G.; Yang, C.; Bai, F.; Shuai, Z.; Wang, L.; Li, Y. *J. Phys. Chem. C.* **2007**, *111*, 8661. (b) Tamayo, A. B.; Dang, X.-D.; Walker, B.; Seo, J.; Kent, T.; Nguyen, T.-Q. *Appl. Phys. Lett.* **2009**, *94*, 103301. (c) Bronstein, H.; Chen, Z.; Ashraf, R.; Zhang, W.; Du, J.; Durrant, J.; Tuladhar, P.; Song, K.; Watkins, S.; Geerts, Y.; Wiennk, M.; Janssen, R.; Anthopoulos, T.; Sirringhaus, H.; Heeney, M.; McCulloch, I. *J. Am. Chem. Soc.* **2011**, *133*, 3272. (d) Yuan, M.; Yin, X.; Zheng, H.; Ouyang, C.; Zuo, Z.; Liu, H.; Li, Y. *Chem-An Asian J.* **2009**, *4*, 707.
(11) (a) Yuan, M.; Rice, A. H.; Luscombe, C. K. *J. Polym. Sci., Part A: Polym. Chem.* **2011**, *49*, 701. (b) Zhang, J.; Cai, W.; Huang, F.; Wang, E.; Zhong, C.; Liu, S.; Wang, M.; Duan, C.; Yang, T.; Cao, Y. *Macromolecules* **2011**, *44*, 894.
(12) (a) Chen, C.-H.; Hsieh, C.-H.; Dubosc, M.; Cheng, Y -J.; Hsu, C.-S. *Macromolecules* **2009**, *43*, 697. (b) Wang, M.; Hu, X.; Liu, P.; Li, W.; Gong, X.; Huang, F.; Cao, Y. *J. Am. Chem. Soc.* **2011**, *133*, 9638.
(13) Cates, N. C.; Gysel, R.; Beiley, Z.; Miller, C. E.; Toney, M. F.; Heeney, M.; McCulloch, I.; McGehee, M. D. *Nano Lett.* **2009**, *9*, 4153.
(14) Cates, N. C.; Gysel, R.; Dahl, J. E. P.; Sellinger, A.; McGehee, M. D. *Chem. Mater.* **2010**, *22*, 3543.
(15) Mayer, A. C.; Toney, M. F.; Scully, S. R.; Rivnay, J.; Brabec, C. J.; Scharber, M.; Koppe, M.; Heeney, M.; McCulloch, I.; McGehee, M. D. *Adv. Funct. Mater.* **2009**, *19*, 1173.
(16) Huo, L.; Hou, J.; Zhang, S.; Chen, H.-Y.; Yang, Y. *Angew. Chem., Int. Ed.* **2010**, *49*, 1500.
(17) Mihailetchi, V. D.; Xie, H. X.; de Boer, B.; Koster, L. J. A.; Blöm, P. W. M. *Adv. Funct. Mater.* **2006**, *16*, 699.
(18) Chan, K. L.; McKiernan, M. J.; Towns, C. R.; Holmes, A. B. *J. Am. Chem. Soc.* **2005**, *127*, 7662.
(19) Welch, G. C.; Bazan, G. C. *J. Am. Chem. Soc.* **2011**, *133*, 4632.